



## Original Article

# An Intraoral Miniature X-ray Tube Based on Carbon Nanotubes for Dental Radiography

Hyun Jin Kim, Hyun Nam Kim, Hamid Saeed Raza, Han Beom Park, and Sung Oh Cho\*

Department of Nuclear and Quantum Engineering, Korea Advanced Institute of Science and Technology, Daejeon 305-701, Republic of Korea

## ARTICLE INFO

## Article history:

Received 18 November 2015

Accepted 11 January 2016

Available online 8 February 2016

## Keywords:

CNT Field Emitter

Miniature X-ray Tube

Radiography

X-ray Image

## ABSTRACT

A miniature X-ray tube based on a carbon-nanotube electron emitter has been employed for the application to a dental radiography. The miniature X-ray tube has an outer diameter of 7 mm and a length of 47 mm. The miniature X-ray tube is operated in a negative high-voltage mode in which the X-ray target is electrically grounded. In addition, X-rays are generated only to the teeth directions using a collimator while X-rays generated to other directions are shielded. Hence, the X-ray tube can be safely inserted into a human mouth. Using the intra-oral X-ray tube, a dental radiography is demonstrated where the positions of an X-ray source and a sensor are reversed compared with a conventional dental radiography system. X-ray images of five neighboring teeth are obtained and, furthermore, both left and right molar images are achieved by a single X-ray shot of the miniature X-ray tube. Copyright © 2016, Published by Elsevier Korea LLC on behalf of Korean Nuclear Society. This is an open access article under the CC BY-NC-ND license (<http://creativecommons.org/licenses/by-nc-nd/4.0/>).

## 1. Introduction

X-rays are widely used for dental imaging to diagnose dental structures, bone loss, and cavities. There are three main types of dental X-ray system: radiography, panorama, and computed tomography [1]. Dental radiography is popularly used to investigate the status of teeth and gums because it provides higher quality X-ray images with lower X-ray doses than dental panorama and computed tomography systems [2–6]. However, in current dental radiography systems, X-rays are irradiated from an X-ray tube outside the mouth next to teeth, while another X-ray sensor is placed inside

the mouth (Fig. 1A). As a consequence, small-sized X-ray sensors are needed for insertion into the mouth and, thereby, the number of teeth that can be radiographically imaged is limited. Normally, images of two whole teeth are obtained by a single X-ray shot with the current dental radiography system that employs an intra-oral sensor (an X-ray sensor placed inside the mouth) and an extra-oral X-ray tube (an X-ray tube placed outside the mouth) [1,7]. Moreover, at least two X-ray shots are required to get images of teeth from both sides of the mouth.

In order to overcome the disadvantages of conventional dental radiography, a novel dental radiograph has been

\* Corresponding author.

E-mail address: [socho@kaist.ac.kr](mailto:socho@kaist.ac.kr) (S.O. Cho).  
<http://dx.doi.org/10.1016/j.net.2016.01.012>

1738-5733/Copyright © 2016, Published by Elsevier Korea LLC on behalf of Korean Nuclear Society. This is an open access article under the CC BY-NC-ND license (<http://creativecommons.org/licenses/by-nc-nd/4.0/>).

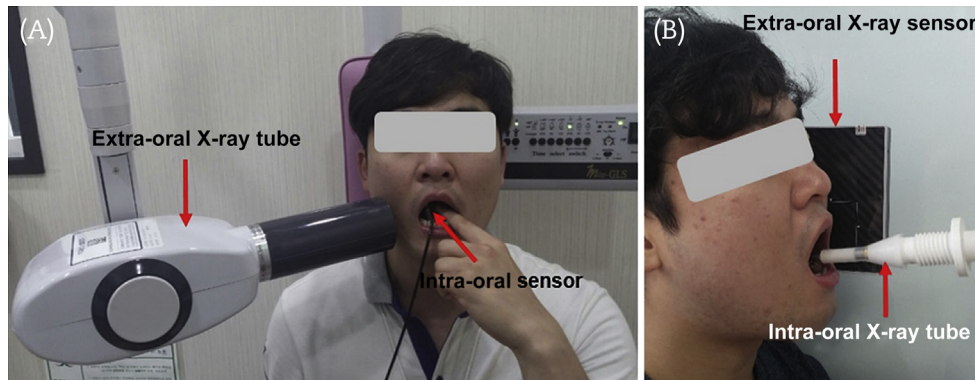


**Fig. 1 – Radiography. (A) Conventional dental radiography consisting of an intra-oral sensor and an extra-oral X-ray tube. (B) A novel dental radiography based on a carbon nanotube-based intra-oral miniature X-ray tube and extra-oral X-ray sensor.**

proposed in which an X-ray source is used inside the mouth while an X-ray sensor is used outside the mouth [8,9]. The intra-oral dental radiograph requires an X-ray source small enough to safely insert into the mouth (Fig. 1B). Recently, we developed a miniature X-ray tube with a diameter of 10 mm and a total length of less than 50 mm [10,11]. The miniature X-ray tube is based on a carbon nanotube (CNT) field emitter and does not require a vacuum pump for its operation. Compared with miniature X-ray tubes based on thermionic electron sources, the CNT-based miniature X-ray tube has a few advantages, including having a higher emission current, better stability, and longer lifetime [10–16]. Moreover, no cooling component is necessary in the CNT-based miniature X-ray tube because heat is not generated from a CNT electron emitter, unlike thermionic electron sources [17–19]. Furthermore, the temperature of the X-ray target can be kept low enough by operating the X-ray tube in a pulse mode. Therefore, the CNT-based miniature X-ray tube can be a good intra-oral X-ray source for the new dental radiography system. Here, we have developed a smaller CNT-based miniature X-ray tube with a diameter of 7 mm, which is a proper intra-oral X-ray source. We present a new dental radiography comprising the miniature X-ray tube and an extra-oral X-ray sensor (Fig. 1B), and show the performance of the dental radiography system. In particular, the dental radiography system was designed to enable a large number of teeth to be radiographically imaged. Furthermore, images of the teeth on both sides of the mouth are simultaneously obtained by a single X-ray shot.

## 2. Materials and methods

A schematic diagram of the CNT-based miniaturized X-ray tube is shown in Fig. 2A. The miniature X-ray tube has a diode structure, which consists of a CNT emitter as a cathode and an X-ray target as an anode. The CNT emitter was fabricated by attaching single-walled CNTs (model: CNT SP95, Carbon Nano-material Technology Co., Pohang, South Korea) to a 0.8-mm copper wire substrate using metal nanoparticles as a binder [20,21]. The CNT emitter was installed inside a focusing electrode, which prevents the divergence of an electron beam generated at the CNT

emitter. The geometrical shape of the focusing electrode was optimized by calculating electron trajectories from the CNT emitter to the X-ray target with an EGN2 code (GA and WB Hermannsfeldt, Los Altos, CA, USA) [22]. The X-ray target has a conical-shaped transmission type. The shape of the target was designed to produce X-rays over large angles with the use of Monte Carlo N-Particle Transport code [23]. The transmission-type target was prepared by coating tungsten, at a thickness of approximately 1.5  $\mu\text{m}$ , on a conical-shaped beryllium window using a magnetron sputtering device.

An alumina ceramic tube, with an inner diameter of 5 mm, an outer diameter of 7 mm, and a length of 30 mm, was used for high-voltage insulation between the cathode assembly and the X-ray target. The focusing electrode, the ceramic tube, and the X-ray target were tightly assembled in a brazing furnace. The brazing process was carried out in a vacuum at a maximum temperature of 720  $^{\circ}\text{C}$  for 5 minutes. Before the brazing process, the alumina ceramic and the focusing electrode were baked at 500  $^{\circ}\text{C}$  for 10 hours. A strip of non-evaporable getter (Model: SP122 SP Getter, SAES Group, Milan, Italy) was used to evacuate the inside of the miniature X-ray tube. It is difficult to tightly vacuum to connect the alumina ceramic and the beryllium window through brazing due to the difference in the thermal expansion coefficients of the two materials [24]. Hence, a cylindrical kovar that has a thermal expansion coefficient similar to that of alumina ceramic was inserted between the alumina ceramic tube and the X-ray target. For the same reason, the focusing electrode was also made of kovar. Fig. 2B displays all the components of the miniature X-ray tube and Fig. 2C shows the final fabricated miniaturized X-ray tube. The outer diameter of the fabricated miniature X-ray tube is 7 mm and the length of the X-ray tube is 47 mm.

The X-ray tubes were operated in a negative high-voltage mode; the cathode was applied to a negative high voltage, while the anode was electrically grounded. The cathode was connected to a commercialized high-voltage connector (model: Claymount CA3, Claymount Co., Ltd., Dinxperlo, The Netherlands). Since the X-ray tubes should be inserted into the mouth, the mouth is exposed to a high voltage, leading to a high-voltage safety issue. To protect the human body from the high voltage, the whole X-ray

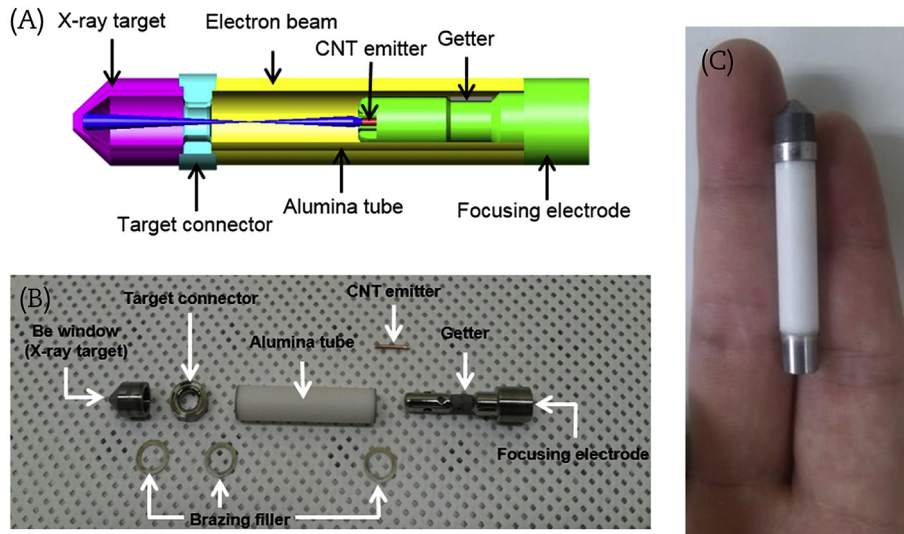


**Fig. 2 – The X-ray tube. (A) Schematic layout of the carbon nanotube-based miniature X-ray tube. (B) Photo showing all the components of the miniature X-ray tube. (C) Photo of the fabricated miniature X-ray tube.**

tube except the X-ray target was covered with a 2-mm-thick layer of silicone rubber that has good electrical insulation properties (Fig. 3A). Due to the silicone rubber coverage, the total diameter of the miniature X-ray tube was increased to 11 mm; however, this diameter is still small enough for the insertion of the X-ray tube into a human mouth.

X-rays were produced in all directions from the conical-shaped transmission target (the detailed angular distribution of the produced X-rays is described in Section 3.1). However, the field of view and the direction of the irradiated X-rays were controlled by a collimator made of copper (Fig. 3B). The collimator also shields unwanted X-rays. The required thickness of the collimator to block unwanted X-rays was determined by calculating the X-ray dose rate using Monte Carlo N-Particle Transport code [18]. The tube voltage is 50 kV and the electron beam current is 200  $\mu\text{A}$  in the calculation. X-ray dose rate is drastically decreased as the copper thickness is increased (Fig. 3C). The calculation confirms that X-rays are almost perfectly blocked when the thickness of the copper collimator

is 3 mm. Following the calculation results, two different copper collimators with a single hole and double holes in opposite directions were fabricated. The hole shape was rectangular and the size of the hole was 9.0 mm  $\times$  10.2 mm.

### 3. Results

#### 3.1. Operational characteristics of the miniature X-ray tube

The angular distribution of the X-rays generated from the miniature tube was measured with a Gafchromic EBT3 film (International Specialty Products, Wayne, NJ, USA) [25]. A cylindrical-shaped aluminum support was used to fix the film and the distance between the target of the miniature X-ray tube and the film can be changed from 1 cm to 5 cm (Fig. 4A). The degree of transparency of the film is decreased as the X-ray dose is increased due to the color change of the film. After the X-ray exposure, the irradiated film was scanned in a

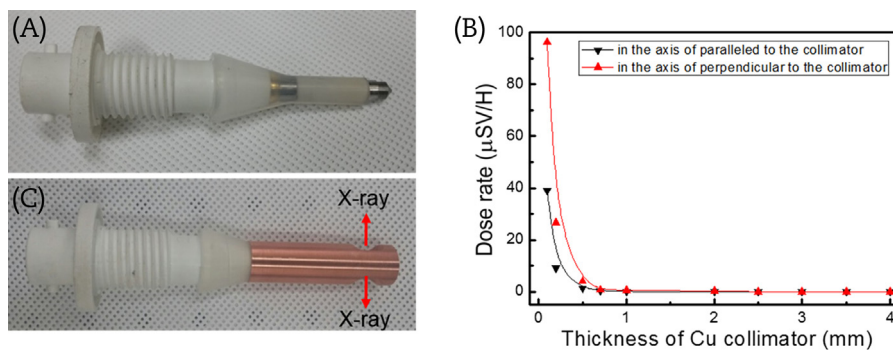


**Fig. 3 – X-ray and dose rate. (A) Miniature X-ray tube covered with silicone rubber. (B) Miniature X-ray tube with a collimator. (C) Calculated dose rate at two different directions as a function of copper thickness. (▲) and (▼) correspond to 0° and 90° to the beam axis, respectively.**

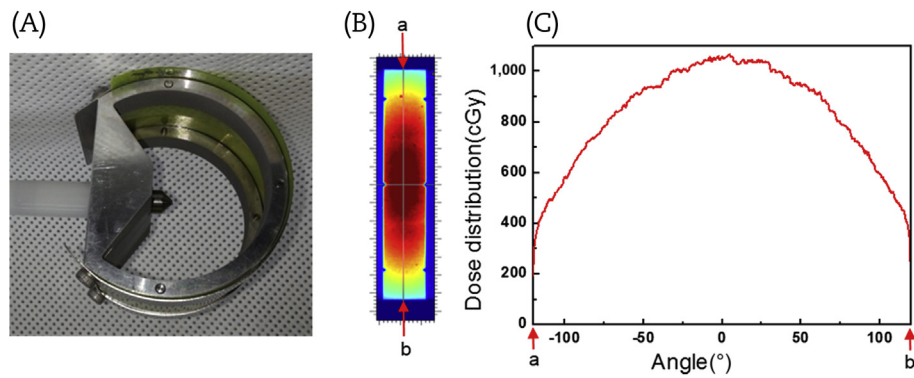


**Fig. 4 – Apparatus and X-ray distribution. (A) Experimental apparatus to measure the angular distribution of the X-rays generated from the carbon nanotube-based miniature X-ray tube. (B) Scanned image of a Gafchromic EBT3 film irradiated by X-rays. (C) Angular X-ray distribution analyzed along the line a–b in (B).**

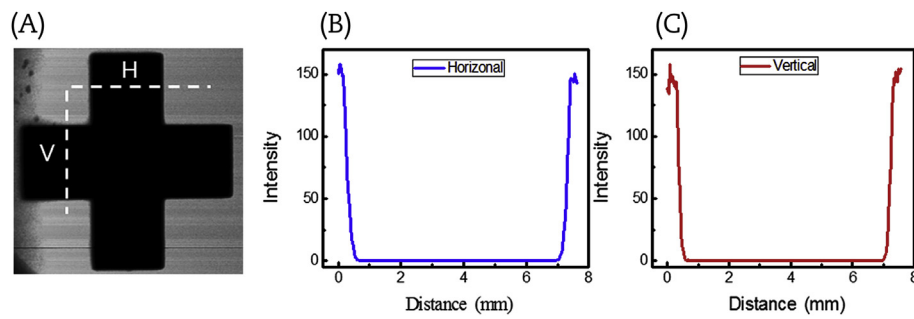


**Fig. 5 – X-ray and intensity profiles. (A) X-ray image of the tungsten cross phantom with magnification of 1.25. (B and C) X-ray intensity profiles along the horizontal (B) and vertical (C) lines in (A), respectively. H, horizontal; V, vertical.**

transmission mode with an Epson Expression 10000XL flatbed scanner (Seiko Epson Corp., Nagano, Japan). The scanned images were recorded and analyzed with the OmniPro™mRT software (version 1.6, IBA Dosimetry, Schwarzenbruck, Germany), giving the relative X-ray intensity at certain positions or the angular distribution of the X-rays. Fig. 4B shows the scanned image of the irradiated film at 3-cm apart from the center of the X-ray target. The miniature X-ray tube was operated at 50 kV. Fig. 4C displays the corresponding angular distribution of the X-rays. The X-ray intensity was maximum at  $0^\circ$  and gradually decreased with the increase in the angle. Here, the angle is defined by the direction with respect to the axis of an electron beam hitting the X-ray target. The dose rate of the X-ray at 3-cm apart from the miniature X-ray tube in air was 8.19 Gy/min at  $0^\circ$  when the X-ray tube was operated at 50 kV with the emission beam current of 140  $\mu$ A. The X-ray intensity at  $90^\circ$  was reduced to 67% of the intensity at  $0^\circ$ . However, this value at  $90^\circ$  is still high enough to get an X-ray radiographic image of the teeth.

In addition, the X-ray focal spot size was measured following the European standard EN 12543-5 [26]. A customized cross phantom made of 0.1-mm-thick tungsten was used for the measurement of the X-ray focal spot sizes in both vertical and horizontal directions. The X-ray image of the tungsten cross phantom taken at 50 kV with the

magnification factor of 1.25 is shown in Fig. 5A. The intensity profiles of the X-ray images were analyzed in both horizontal and vertical directions (Figs. 5B and 5C). From the intensity profiles, X-ray focal spot sizes were calculated to be 0.67 mm in the horizontal direction and 0.48 mm in the vertical direction. These values are comparable to the focal spot sizes of commercialized X-ray tubes for conventional dental X-ray radiography, suggesting that dental X-ray images of good quality can be achieved using the fabricated miniature X-ray tube.

### 3.2. X-ray radiography using the intra-oral miniature X-ray tube

Using the fabricated CNT-based miniature X-ray tube as an intra-oral X-ray source, X-ray radiographic images of a human teeth phantom were achieved. The human teeth phantom was composed of a 7-mm bolus and six teeth. A CMOS photodiode array detector (model: Vatech Xmaru0505CF, Humanray Co., Ltd., Gyeonggi-do, South Korea) with a pixel pitch of 35  $\mu$ m was used as an X-ray sensor. The active area of the X-ray detector was 48.0 mm  $\times$  54.0 mm. The distance between the target of the miniature X-ray tube and the X-ray detector was 7 cm and the teeth phantom was attached to the detector. A collimator with a hole was used to get the X-ray

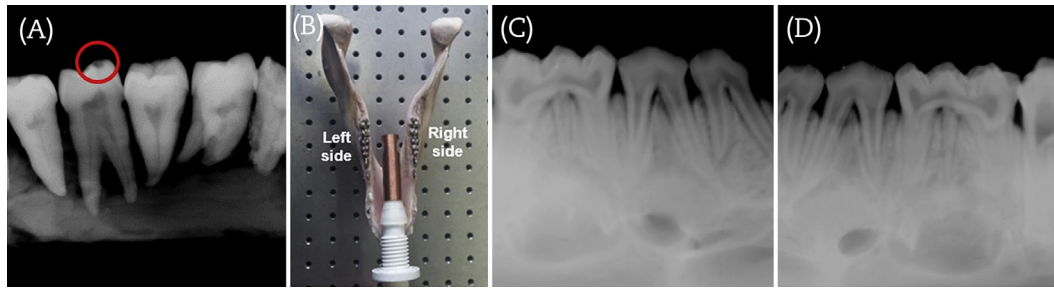


**Fig. 6 – X-ray images of teeth. (A) X-ray image of a human teeth phantom using the intra-oral X-ray tube. The red circle indicates a dental caries. (B) Experimental platform to take X-ray images of the pig teeth specimen. (C and D) X-ray images of left (C) and right (D) pig teeth, respectively.**

images. Fig. 6A shows an X-ray image of the human teeth phantom using the intra-oral X-ray tube. The miniature X-ray tube was operated at 50 kV and the exposure time was 0.1 seconds. Comparatively high-quality X-ray images were obtained with the intra-oral miniature X-ray tube. Pulp cavities, enamel, and dentin are clearly distinguished and a dental caries is also observed. In addition, as an X-ray sensor is inserted in a mouth in conventional dental radiography, the size of the X-ray sensor is limited (normally less than  $3\text{ cm} \times 4\text{ cm}$ ). Thus, images of only one to three whole teeth can be achieved using a conventional dental radiography. However, an image of five whole teeth was obtained by a single X-ray shot using the intra-oral X-ray tube. Our radiography scheme employs an intra-oral X-ray tube and extra-oral X-ray sensors. Since X-ray sensors are placed outside the mouth, large-sized X-ray sensors can be used to get the radiographic images. The size of the X-ray sensor used in the present experiments was  $48.0\text{ mm} \times 54.0\text{ mm}$ , and thereby, only five teeth were imaged. However, if a larger X-ray sensor was used, a larger number of teeth images could be achieved. This is one of the advantages of the novel X-ray dental radiography employing an intra-oral miniature X-ray tube and extra-oral X-ray sensors.

In addition, the new dental radiography allows to X-ray images of the teeth at both ends to be achieved simultaneously by a single X-ray shot. To demonstrate this, a pig teeth specimen extracted from a lower jaw bone was used for the X-ray radiography. The CNT-based miniature X-ray tube was inserted into the pig teeth specimen and two X-ray sensors (Vatech Xmaru0505CF, Humanray Co., Ltd., Gyeonggi-do, South Korea) were placed outside of the teeth near the left and right molars (Fig. 6B). A collimator with two holes (hole size:  $9\text{ mm} \times 10.2\text{ mm}$ ) at opposite directions was used to get the radiographic images. The CNT-based miniature X-ray tube was operated at 50 kV and the exposure time was 0.1 seconds. Figs. 6C and 6D show left and right teeth images of the pig teeth specimen, respectively. The teeth, root canals, and jaw bones at both sides are clearly observed in the X-ray images. The left and right teeth images were obtained by a single X-ray shot. The fact that many teeth at left and right sides can be radiographically imaged simultaneously by a single X-ray shot is also one of the advantages of the novel X-ray dental radiography employing an intra-oral miniature X-ray tube and extra-oral X-ray sensors.

#### 4. Discussion

We have demonstrated a dental radiography system that employs an intra-oral CNT-based miniature X-ray tube and extra-oral X-ray sensors. The X-ray tube can be safely inserted into a mouth due to its small diameter and a cover of insulation material for high-voltage protection. X-rays are produced only in the direction of teeth, while other directions are shielded by a collimator. Using the intra-oral miniature X-ray tube, an X-ray image of five teeth was successfully obtained. Moreover, images of left and right teeth were simultaneously obtained by a single X-ray shot. These results show that the novel dental radiograph, which employs a miniature intra-oral X-ray tube, performs better than conventional dental radiography, which uses a large extra-oral X-ray tube.

#### Conflicts of interest

The authors have no conflicts of interest to disclose.

#### Acknowledgments

This work was supported by the National Research Foundation of Korea Grant funded by the Korean Government (number NRF-2015M2A2A4A03045077) and a grant from the Korean Health Industry Development Institute funded by the Ministry of Health and Welfare, Republic of Korea (grant number: HI15C0638).

#### REFERENCES

- [1] L. Li, Z. Chen, Z. Zhao, D. Wu, X-ray digital intra-oral tomosynthesis for quasi-three-dimensional imaging: system, reconstruction algorithm, and experiments, *Opt. Eng.* 52 (2013) 013201.
- [2] K. de Faria Vasconcelos, K.M. Evangelista, C.D. Rodrigues, C. Estrela, T.O. de Sousa, M.A.G. Silva, Detection of periodontal bone loss using cone beam CT and intraoral radiography, *Dentomaxillofac. Radiol.* 41 (2012) 64–69.
- [3] N.S. Venkatesh Babu, P. Patel, Comparative evaluation of extraoral and intraoral periapical radiographic technique in children, *Int. J. Sci. Stud.* 2 (2015) 6–11.

- [4] N. Bagis, M.E. Kolsuz, S. Kursun, K. Orhan, Comparison of intraoral radiography and cone-beam computed tomography for the detection of periodontal defects: an *in vitro* study, *BMC Oral Health* 15 (2015) 64.
- [5] R. Kumar, N. Khambete, E. Priya, Extraoral periapical radiography: an alternative approach to intraoral periapical radiography, *Imaging Sci. Dent.* 41 (2011) 161–165.
- [6] T. Tokuyasu, M. Yamamoto, K. Okamura, K. Yoshiura, A Training Simulator for Intraoral Radiography, 2006 IEEE/RSJ International Conference on IEEE, IEEE, New York, 2006.
- [7] I.A. Pretty, Caries detection and diagnosis: novel technologies, *J. Dent.* 34 (2006) 727–739.
- [8] S.H. Cho, S.Y. Kim, S.H. An, S.M. Lim, R.N. Lee, Feasibility study of insertable miniature x-ray source for dental imaging, *Korean J. Radio.* 6 (2012) 39–45.
- [9] S.H. Cho, D.Y. Kim, K.W. Baek, R.N. Lee, Introduction of Dental X-ray Imaging with New Concept—Intraoral X-ray Tube, *The Magazine of the IEEK* 48, 2011, p. 95.
- [10] S.H. Heo, H.J. Kim, J.M. Ha, S.O. Cho, A vacuum-sealed miniature X-ray tube based on carbon nanotube field emitters, *Nanoscale Res. Lett.* 7 (2012) 258.
- [11] H.J. Kim, J.M. Ha, S.H. Heo, S.O. Cho, Small-sized flat-tip CNT emitters for miniaturized X-ray tubes, *J. Nano.* 2012 (2012). Article ID 854602.
- [12] Y. Sakai, D. Tone, S. Nagatsu, T. Endo, S. Kita, F. Okuyama, Characterization of field emission from carbon nanofibers on a metal tip, *Appl. Phys. Lett.* 95 (2006) 073104.
- [13] N. De Jonge, Y. Lamy, K. Schoots, T.H. Oosterkamp, High brightness electron beam from a multi-walled carbon nanotube, *Nature* 420 (2002) 393–395.
- [14] G. Zhao, J. Zhang, Q. Zhang, J. Tang, O. Zhou, L.C. Qin, Fabrication and test of single nanotube emitter as point electron source, *Microsc. Microanal.* 10 (2004) 550–551.
- [15] G. Zhao, Q. Zhang, H. Zhang, G. Yang, O. Zhou, L.C. Qina, Field emission of electrons from a Cs-doped single carbon nanotube of known chiral indices, *Appl. Phys. Lett.* 89 (2006) 63113.
- [16] S.H. Heo, A. Ihsan, S.O. Cho, Transmission-type microfocus x-ray tube using carbon nanotube field emitters, *Appl. Phys. Lett.* 90 (2007) 183109.
- [17] R.J. Parmee, C.M. Collins, W. Milne, M.T. Cole, X-ray generation using carbon nanotubes, *Nano. Convergence* 2 (2015) 1–27.
- [18] E.L. Murphy, R.H. Good, Thermionic emission, field emission, and the transition region, *Phys. Rev.* 102 (1956) 1464.
- [19] M.J. Rivard, S.D. Davis, L.A. DeWerd, T.W. Rusch, S. Axelrod, Calculated and measured brachytherapy dosimetry parameters in water for the Xofig X-Ray Source: an electronic brachytherapy source, *Med. Phys.* 33 (2006) 4020–4022.
- [20] S.H. Heo, A. Ihsan, S.O. Cho, Stable Field Emitters for a Miniature X-ray tube using carbon nanotube drop drying on a flat metal tip, *Nanoscale Res. Lett.* 5 (2010) 720–724.
- [21] J.M. Ha, H.J. Kim, H.S. Raza, S.O. Cho, Highly stable carbon nanotube field emitters on small metal tips against electrical arcing, *Nanoscale Res. Lett.* 8 (2013) 355.
- [22] W.B. Herrmannsfeldt, G.A. Herrmannsfeldt, EGN Electron Optics Program, SLAC, Stanford, California, 1993.
- [23] Los Alamos National Lab, MCNP-A General Monte Carlo N-Particle Transport, version 5, 2003.
- [24] G.J. Qiao, C.G. Zhang, Z.H. Jin, Thermal cyclic test of alumina/kovar joint brazed by Ni-Ti active filler, *Ceram. Int.* 29 (2003) 7–11.
- [25] G. Massillon, S. Chiu-Tsao, I. Domingo-Munoz, M. Chan, Energy dependence of the new Gafchromic EBT3 film: dose response curves for 50 kV, 6 and 15 MV X-ray beams, *Int. J. Med. Phys. Clin. Eng. Radiat. Oncol.* 1 (2012) 60–65.
- [26] European Committee for Standardization: EN 12543–5, E. Brussels, 1999.